THE JOURNAL OF PHYSICAL CHEMISTRY Letters

Letter

pubs.acs.org/JPCL

# Sulfated Graphene Oxide as a Hole-Extraction Layer in High-Performance Polymer Solar Cells

Jun Liu,[†] Yuhua Xue,[†,‡] and Liming Dai*

Department of Macromolecular Science and Engineering, Case School of Engineering, Case Western Reserve University, 10900 Euclid Avenue, Cleveland, Ohio 44106, United States

Supporting Information

**ABSTRACT:** In this study, we have rationally designed and successfully developed sulfated graphene oxide (GO−$OSO_3H$) with −$OSO_3H$ groups attached to the carbon basal plane of reduced GO surrounded with edge-functionalized −COOH groups. The resultant GO−$OSO_3H$ is demonstrated to be an excellent hole extraction layer (HEL) for polymer solar cells (PSCs) because of its proper work function for Ohmic contact with the donor polymer, its reduced basal plane for improving conductivity, and its −$OSO_3H$/−COOH groups for enhancing solubility for solution processing. Compared with that of GO, the much improved conductivity of GO−$OSO_3H$ (1.3 S $m^{-1}$ vs 0.004 S $m^{-1}$) leads to greatly improved fill factor (0.71 vs 0.58) and power conversion efficiency (4.37% vs 3.34%) of the resulting PSC devices. Moreover, the device performance of GO−$OSO_3H$ is among the best reported for intensively studied poly(3-hexylthiophene):[6,6]-phenyl-C61 butyric acid methyl ester (P3HT:PCBM) devices. Our results imply that judiciously functionalized graphene materials can be used to replace existing HEL materials for specific device applications with outstanding performance.

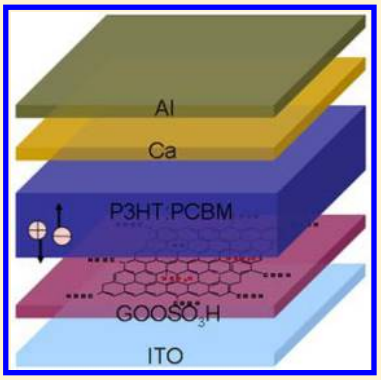


**SECTION:** Energy Conversion and Storage; Energy and Charge Transport

Having a large surface area, high intrinsic charge mobility, good thermal and electrical conductivities, high Young's modulus, and excellent optical transmittance,[1,2] graphene has attracted considerable interest for a large variety of applications, including solar cells, field-effect transistors, light emitting diodes, supercapacitors, fuel cells, sensors, and actuators.[3−8] For many of the aforementioned and other applications, it is highly desirable to tune its chemical and electronic structures to meet the requirements for specific applications. However, it remains a big challenge to chemically functionalize graphene while keeping its basal plane conductivity intact for outstanding performance. Recent work on the edge-functionalization of graphene provides an effective means for the development of functionalized graphene with tailor-made chemical structure and electronic property. However, device applications of the edge-functionalized graphene have hardly been demonstrated.[9−11] Herein, we report the first synthesis of rationally designed sulfated graphene oxide (GO−$OSO_3H$) by substituting the in-plan epoxy and/or hydroxyl groups of graphene oxide (GO) with −$OSO_3H$ groups while retaining its −COOH edge groups, and further demonstrate the use of the resultant GO−$OSO_3H$ as a hole extraction material in polymer solar cells (PSCs) with outstanding device performance.

Owing to their low-cost roll-to-roll production and flexibility, PSCs, consisting of a solution-cast blend of electron donor/acceptor (e.g., poly(3-hexylthiophene):[6,6]-phenyl-C61 butyric acid methyl ester, P3HT:PCBM) sandwiched between cathode and anode, have recently attracted considerable attention as promising clean energy devices.[12−14] Since the interfaces between the active layer and the two electrodes play important roles in regulating the overall photovoltaic efficiency of a PSC, the use of charge extraction layers between the active layer and electrodes become essential.[15,16] The functions of charge extraction layers include minimizing energy barriers for charge carrier extraction, forming a selective contact for holes and blocking electrons at anode and vise versa at cathode, as well as modifying the interfaces to alter the active layer morphology. For a hole extraction layer (HEL), key parameters include high transparency, good stability, and solution processability apart from proper work function, and high conductivity necessary for both HEL and electron extraction layers (EEL). The state-of-the-art hole-extraction material is poly(styrenesulfonate)-doped poly(3,4-ethylenedioxythiophene) (PEDOT:PSS), which can be spin-cast from commercially available aqueous solution. However, PEDOT:PSS is highly acidic (PH = 1−2) and corrosive to indium tin oxide (ITO) anode. Furthermore, it has been reported that solution-deposited PEDOT:PSS films often show inhomogeneous morphology and electrical property,[17,18] leading to a poor long-term stability for PSCs. Consequently, several inorganic semiconductors, such as $V_2O_5$, $MoO_3$, $WO_3$, and NiO, have been investigated to replace PEDOT:PSS.[19−22] However, deposition of these inorganic semiconductors involves vacuum-based elaborate and careful fabrication

**Received:** June 3, 2012
**Accepted:** June 29, 2012

  

**Scheme 1. Synthetic Route to GO−$OSO_3H$**

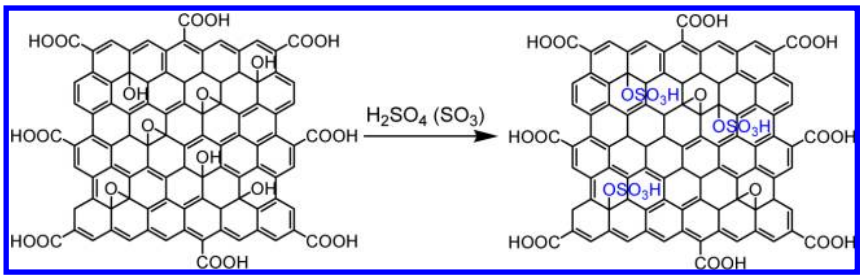


processes, which are incompatible with the low-cost roll-to-roll processing for PSC fabrication.

Recently, GO has been demonstrated to be an efficient hole extraction material for PSCs with long lifetime.[23−27] Being produced by solution oxidation of graphite with acids (e.g., $H_2SO_4$, $HNO_3$), GO consists of graphene sheets with carboxylic acid groups at the edge and epoxy and hydroxyl groups on the basal plane to disrupt conjugation of the hexagonal graphene lattice.[28,29] In spite of the great advantage of low manufacturing cost and compatibility with roll-to-roll processing, GO HEL suffers from low conductivity, and hence a high series resistance, a low fill factor (FF), and low device efficiency. Indeed, PSCs based on a P3HT:PCBM active layer and GO as HEL reported to date all exhibit a FF less than 0.65 and power conversion efficiency (PCE) lower than 4%,[23−27] both of which are much lower than those of the corresponding PEDOT:PSS device.[13,14] To improve the conductivity of the GO layer and to enhance device performance, Gao et al.[25] added single-walled carbon nanotubes to the GO layer and Yeo et al.[26] used *p*-toluenesulfonyl hydrazide to reduce GO.

As far as we are aware, the hole extraction property of GO arises from two factors: (i) doping of the adjacent donor polymer in active layer by periphery −COOH groups of GO to minimize the contact resistance, and (ii) transporting holes through its basal plane to be collected on anode.[23−27] To improve the hole extraction capability of GO, therefore, both the acidicity and the hole transporting capability need to be considered. In this regard, we have rationally designed and successfully developed sulfated GO (i.e., GO−$OSO_3H$) with −$OSO_3H$ groups attached to the carbon basal plane of reduced GO surrounded with edge-functionalized −COOH groups (Scheme 1). We found that the strong acidic −$OSO_3H$ groups in the carbon basal plane of GO−$OSO_3H$, together with −COOH groups along its edge, enhanced the doping of the donor polymer, while the dehydration effect of fuming sulfuric acid ($H_2SO_4$ + 30%$SO_3$) used for the synthesis of GO−$OSO_3H$ reduced the basal plane of GO to largely recover the conjugation for efficient charge transport. The presence of −$OSO_3H$ groups in its basal plane and −COOH groups along its edge further rendered GO−$OSO_3H$ soluble for solution processing.[30,31] As a result, the PSC device based on a P3HT:PCBM active layer and GO−$OSO_3H$ HEL exhibited a FF of 0.71 and PCE of 4.37%, both of which were much higher than those of the corresponding PSCs based on GO HEL and were among the highest values reported for P3HT:PCBM devices.[32] As demonstrated in this study, therefore, the rationally designed GO−$OSO_3H$ HEL material implies that judiciously functionalized graphene materials can be used to replace existing HEL materials for specific device applications with outstanding performance.

Scheme 1 shows the synthetic route to GO−$OSO_3H$. To start with, GO was prepared from graphite following a modified Hummer's method.[8] The dry GO powder was then dispersed and stirred in fuming sulfuric acid (i.e., $H_2SO_4$ + 30%$SO_3$) for 3 days to afford GO−$OSO_3H$. The crude product was repeatedly washed with acetonitrile to remove the excessive acid and to produce the pure GO−$OSO_3H$. Fuming sulfuric acid was a widely used sulfonating (or sulfating) agent for unsaturated hydrocarbons. Along with others, we previously used fuming sulfuric acid to react with fullerenol or carbon nanotubes to form sulfonic groups on these polyaromatic carbon materials.[33−35] Strong acid also have the dehydration capability, leading to partial reduction of GO.[33,34,36,38] Previous studies paved the way for the preparation of GO−$OSO_3H$ in the present work. As illustrated in Scheme 1, a portion of the epoxy groups and hydroxyl groups on the carbon basal plane of GO could be either removed or transformed into sulfate groups through the treatment with fuming sulfuric acid (see below).

The resultant GO−$OSO_3H$ was investigated by X-ray photoelectron spectroscopy (XPS), Raman, Fourier transform infrared spectroscopy (FT-IR), ultraviolet−visible spectroscopy (UV−vis), atomic force microscopy (AFM), scanning electron microscopy (SEM), transmission electron microscopy (TEM), elemental analysis (EA), and thermogravimetric analysis (TGA). Figure 1a shows a typical AFM image for GO−$OSO_3H$ on a silica substrate, along with the corresponding height profiles. As can be seen, the thickness of GO−$OSO_3H$ is about 1.2 nm, very close to that of GO, indicating the presence of single-layer graphene sheets in GO−$OSO_3H$. This has also been confirmed by the SEM and TEM images shown in Figure S1. EA and XPS measurements reveal the presence of −$OSO_3H$ groups in GO−$OSO_3H$. The content of S in GO−$OSO_3H$ was estimated to be 4.49 wt % by EA or to be 1.2 atom % by XPS (Figure 1b).

The pH value of 0.2 mg/mL aqueous solution of GO−$OSO_3H$ (pH = 3.09) is lower than that of GO (pH = 3.93) due to the presence of strong acidic −$OSO_3H$ groups in GO−$OSO_3H$. Figure S2 (Supporting Information) presents the titration curves of GO−$OSO_3H$ and GO. In the titration curve of GO, there is two-step gradual pH increase when adding NaOH solution. The pH range of 4−7 is mainly attributed to the dissociation of −COOH groups, while the pH range of 7−10 is mainly due to the dissociation of hydroxyl groups in GO. By contrast, for the titration curve of GO−$OSO_3H$, there is only a one-step abrupt pH increase because of the presence of the −COOH groups and the −$OSO_3H$ groups as well as the absence of hydroxyl groups. The titration curve difference of GO and GO−$OSO_3H$ is also evidence for the transformation of hydroxyl groups to −$OSO_3H$ groups in GO−$OSO_3H$. The amount of base exchangeable protons in GO−$OSO_3H$ (from −$OSO_3H$ groups and −COOH groups) is 5.86 mmol/g at the


dx.doi.org/10.1021/jz300723h | *J. Phys. Chem. Lett.* 2012, 3, 1928−1933

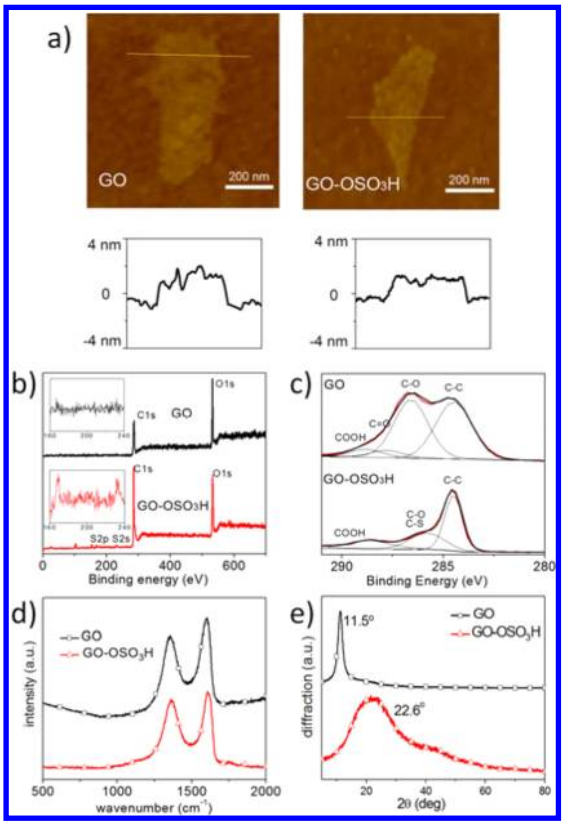


**Figure 1.** AFM images and height profiles on Si substrates (a), XPS survey spectra (b), high-resolution XPS C1s spectra (c), Raman spectra (d), and XRD profiles (e) of GO−$OSO_3H$ and GO. The insets in panel b show the magnified region from 160 to 240 eV.

titration point of pH = 10, which is 1.86 times higher than that of GO (from −COOH groups and hydroxyl groups).

The basal plane of GO−$OSO_3H$ is more reduced than that of GO according to XPS (Figure 1b,c), Raman (Figure 1d), XRD (Figure 1e), and UV/vis (Figure S3) results. As shown by the high-resolution C1s spectra in Figure 1c, GO−$OSO_3H$ exhibits a significantly weaker C−O peak than that of GO, indicating an effective conversion of the epoxy/hydroxyl groups in GO into $-OSO_3H$ in GO−$OSO_3H$. The less oxygen content of GO−$OSO_3H$ (O content: 28.8 atom %) than that of GO (O content: 37.3 atom %) as shown in Figure 1b suggests that the transformation from epoxy/hydroxyl to $-OSO_3H$ in the presence of fuming sulfuric acid is accompanied by basal plane reduction. Figure 1d reproduces the Raman spectra of the GO material before and after the sulfonation, which shows a slightly higher intensity ratio of the D-band to G-band ($I_D/I_G$) for GO−$OSO_3H$ ($I_D/I_G$ = 0.88) than that for GO ($I_D/I_G$ = 0.79). The observed increase in the $I_D/I_G$ ratio upon sulfonation is due to the reduction of the basal plane to produce more $sp^2$ C domains but with a small size.[37] The corresponding XRD patterns given in Figure 1e show a peak shift from $2\theta = 11.50°$ ($d$ = 7.65 Å) for GO to $2\theta = 26.40°$ ($d$ = 3.91 Å) for GO−$OSO_3H$, implying that the largely exfoliated GO sheets partially restacked through $\pi-\pi$ interaction upon sulfonation. This result also supports the removal of functional groups from the basal plane and reduction of the basal plane. The sulfonation-induced basal plane reduction is also evidenced by the redshift seen in the UV/vis absorption spectrum of GO−$OSO_3H$ compared to that of GO (Figure S3a) as well as the color change from brownish GO to black GO−$OSO_3H$ shown in Figure S3b.

Prior to the use of GO−$OSO_3H$ as a hole extraction material in PSCs, we measured the work function of GO−$OSO_3H$ by Kelvin probe force microscopy to be −4.8 eV. This value matches the highest occupied molecular orbital (HOMO) level of P3HT (−5.0 eV) for an Ohmic contact. As mentioned earlier, the presence of the $-OSO_3H$/−COOH groups in GO−$OSO_3H$ can lead to the surface doping of P3HT to minimize the contact resistance. The surface doping of P3HT by GO−$OSO_3H$ is verified by the subtle difference between the optical absorbance of a GO−$OSO_3H$/P3HT bilayer and the sum absorbance of an individual P3HT layer and an individual GO−$OSO_3H$ layer with the same thicknesses. As seen in Figure S6, the bilayer exhibits stronger absorption at ca. 800 nm attributed to the doped P3HT, and weaker absorption below 550 nm attributable to the pristine P3HT, indicating the doping of P3HT at the GO−$OSO_3H$/P3HT interface. Furthermore, the reduced basal plane in GO−$OSO_3H$ greatly improves the conductivity of GO−$OSO_3H$ up to about 400 times higher than that of GO (1.3 S/m for GO−$OSO_3H$ vs 0.004 S/m for GO, Table 1). The increased conductivity is expected to reduce the

**Table 1. Characteristics of PEDOT:PSS, GO and GO−$OSO_3H$**

| HEL | conductivity (S $m^{-1}$) | work function (eV) | contact angle (°) |
|---|---|---|---|
| PEDOT:PSS | 0.1[a] | 5.2[a] | 14.8 |
| GO | 0.004 | 4.7 | 36.5 |
| GO−$OSO_3H$ | 1.3 | 4.8 | 81.0 |

[a]adopted from www.clevios.com.

series resistance and increase the PCE of the resulting PSC devices. Due to the presence of $-OSO_3H$ groups, GO−$OSO_3H$ also exhibits good solubility in polar organic solvents (e.g., dimethylformamide, DMF), making the solution processing feasible. In contrast, it has been widely reported that reduced GO with an insufficient number of oxygen groups on the basal plane tends to form large aggregates in solution, which cannot be used to produce thin uniform films by spincoating.[28,29] The AFM image given in Figure S7 shows a uniform surface with no aggregate for a thin film spincast from a 0.5 mg/mL DMF solution of GO−$OSO_3H$. Owing to the reduced basal plane, GO−$OSO_3H$ turns out to be more hydrophobic than GO, as revealed by the larger water contact angle (81.0° for GO−$OSO_3H$ vs 36.5° for GO) shown in Figure S8. The improved hydrophobicity can enhance the contact between the HEL and the active layer to facilitate the hole transport. All the features described above imply that GO−$OSO_3H$ should be an attractive hole extraction material.

To evaluate the performance of GO−$OSO_3H$ as HEL, we fabricated three PSC devices with the configuration of ITO/HEL/P3HT:PCBM(200 nm)/Ca(20 nm)/Al(100 nm). The GO−$OSO_3H$ layer was spincoated from its 0.5 mg/mL solution in DMF. The HELs (thicknesses) in these devices are PEDOT:PSS (25 nm), GO (2 nm), and GO−$OSO_3H$ (2 nm), respectively. Figure 2a shows the current density−voltage ($J-V$) curves measured from these devices under AM1.5G illumination with the numerical data listed in Table 2. As can be seen, the reference device with PEDOT:PSS exhibits a open-circuit voltage ($V_{OC}$) of 0.60 V, short-circuit current density ($J_{SC}$) of 10.35 mA/$cm^2$, FF of 0.71 and PCE of 4.39%. For


dx.doi.org/10.1021/jz300723h | J. Phys. Chem. Lett. 2012, 3, 1928−1933

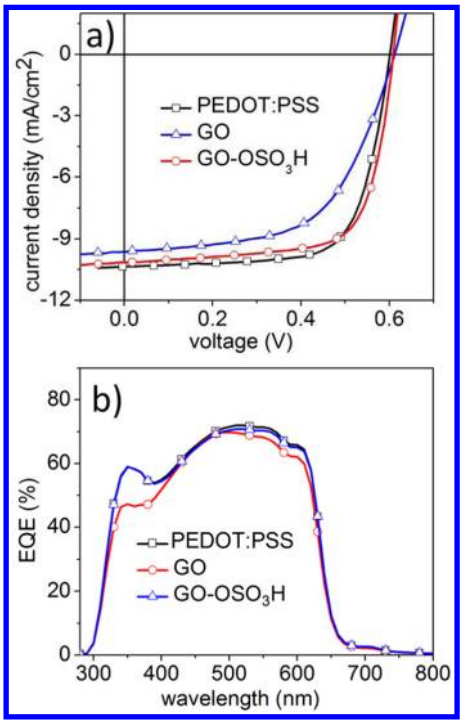


**Figure 2.** Current density–voltage curves (a) and EQE spectra (b) of the PSC devices with PEDOT:PSS (25 nm), GO (2 nm), or GO–$OSO_3H$ (2 nm) as the HEL.

**Table 2. Characteristics of the PSC Devices Studied in This Work**

| HEL | thickness (nm) | $V_{OC}$ (V) | $J_{SC}$ (mA/cm$^2$) | FF | PCE (%) | $R_s$ (Ω cm$^2$) |
|---|---|---|---|---|---|---|
| PEDOT:PSS | 25 | 0.60 | 10.35 | 0.71 | 4.39 | 1.4 |
| GO | 2 | 0.61 | 9.64 | 0.58 | 3.34 | 3.1 |
| GO | 4 | 0.61 | 9.15 | 0.55 | 3.04 | 4.7 |
| GO | 6 | 0.61 | 8.79 | 0.48 | 2.66 | 6.4 |
| GO–$OSO_3H$ | 2 | 0.61 | 10.15 | 0.71 | 4.37 | 1.2 |
| GO–$OSO_3H$ | 4 | 0.61 | 11.16 | 0.68 | 4.27 | 1.4 |
| GO–$OSO_3H$ | 6 | 0.61 | 10.13 | 0.67 | 4.23 | 1.7 |

comparison, the device with GO exhibits a $V_{OC}$ of 0.61 V, $J_{SC}$ of 9.64 mA/cm$^2$, and FF of 0.58, leading to PCE of 3.34%. The relatively poor photovoltaic performance observed for the GO device can be attributed to the high series resistance (Table 2) associated with the insulating GO. By contrast, the device based on GO–$OSO_3H$ shows a $V_{OC}$ of 0.61 V, $J_{SC}$ of 10.15 mA/cm$^2$, FF of 0.71, and PCE of 4.37%. Compared with the GO-based device, its GO–$OSO_3H$ counterpart exhibits a much lower series resistance ($R_S$) (1.2 Ω cm$^2$ vs 3.1 Ω cm$^2$), and hence a significantly improved FF (0.71 vs 0.58) and PCE (4.37% vs 3.34%). In a good consistency with the $J$–$V$ curves in Figure 2a, the external quantum efficiency (EQE) spectra given in Figure 2b also implies that the overall performance of GO–$OSO_3H$ HEL is fairly comparable to that of PEDOT:PSS. In particular, both the FF and PCE of the GO–$OSO_3H$ device are higher than the reported values for many of the intensively studied P3HT:PCBM-based PSCs.[34] Therefore, GO–$OSO_3H$ is an excellent hole extraction material.

The performance of PSCs with graphene-based HELs were further optimized by changing the thickness of the GO or GO–$OSO_3H$ HEL (Figure 3, Table 2). As can be seen in Figure 3b, the photovoltaic performance of the GO-based device depends

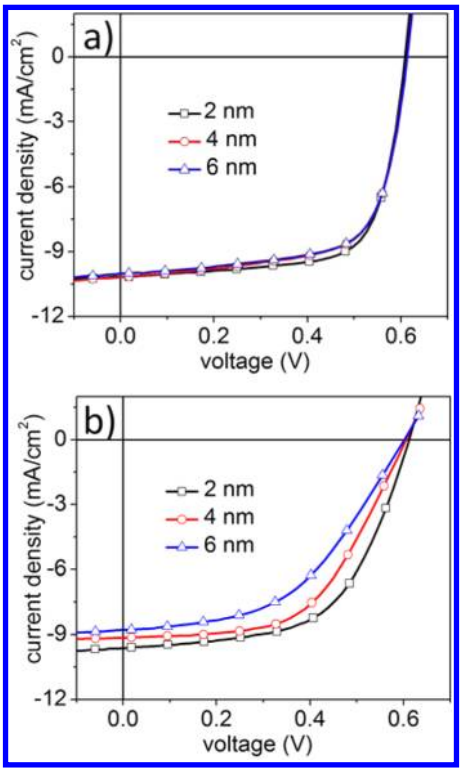


**Figure 3.** Current density–voltage curves of the PSC devices with GO–$OSO_3H$ (a) or GO (b) as the HEL with different thicknesses.

strongly on the GO layer thickness. Because of the poor conductivity of GO, an increase in the GO thickness from 2 to 6 nm increases the series resistance from 3.1 to 6.4 Ω cm$^2$, and hence the FF decreases from 0.58 to 0.48, and the PCE decreases from 3.34% to 2.66% (Table 2). By contrast, the performance of the GO–$OSO_3H$-based device is nearly independent of the HEL thickness over the GO–$OSO_3H$ layer thickness range from 2 to 6 nm (Figure 3a). These results confirm, once again, that the improved conductivity associated with the reduced basal plane plays an important role in ensuring the excellent hole extraction performance for GO–$OSO_3H$.

In conclusion, we have rationally designed and prepared GO–$OSO_3H$ with $-OSO_3H$ groups introduced to the reduced basal plane of GO and −COOH groups along its edge. The resultant GO–$OSO_3H$ has been demonstrated to be an excellent hole extraction material for PSCs. This is because the well-matched work function between GO–$OSO_3H$ and P3HT and the interfacial doping of P3HT by GO–$OSO_3H$ have not only ensured Ohmic contacts for the HEL and active layer but also improved conductivity of the HEL to reduce the series resistance. Therefore, the rationally designed GO–$OSO_3H$ with outstanding performance as a hole extraction material demonstrated in this study represents a significant step forward to practical use of graphene materials for tuning interfacial properties in PSCs to achieve excellent device performance.

## EXPERIMENTAL METHODS

*Synthesis of GO–$OSO_3H$.* GO was prepared from graphite powder according to a modified Hummer's method as reported elsewhere.[8] Aqueous solution of GO (0.5 mg/mL, 20 mL) was filtrated through a 0.2-$\mu$m PVDF membrane. The filtrated GO


dx.doi.org/10.1021/jz300723h | J. Phys. Chem. Lett. 2012, 3, 1928–1933

powder was then dispersed in diethyl ether and centrifuged repeatedly three times, followed by vacuum drying at 40 °C overnight. A mixture of GO (10 mg) and fuming sulfuric acid (3 mL) was stirred at room temperature under $N_2$ atmosphere for 3 days to give a dark brown suspension, which was added dropwise into anhydrous diethyl ether (40 mL) with vigorous stirring in an ice bath. The precipitates were separated from solution through centrifugation. The solid was purified by repeated dispersing in diethylether and centrifuging, and then dried in vacuum at 40 °C overnight to afford GO−$OSO_3H$ as a dark solid. Yield: 10 mg.

## ■ ASSOCIATED CONTENT

### Ⓢ Supporting Information

Instrument and characterization, device fabrication and characterization, SEM and TEM images, titration curves, FT-IR spectra, TGA curves, UV/vis absorption spectra, contact angle images, and AFM images. This material is available free of charge via the Internet at http://pubs.acs.org.

## ■ AUTHOR INFORMATION

### Corresponding Author

*E-mail: liming.dai@case.edu.

### Author Contributions

†These authors contributed equally.

### Notes

The authors declare no competing financial interest.

‡On leave from the School of Ophthalmology & Optometry, Wenzhou Medical College, Zhejiang 325027 (P. R. China).

## ■ ACKNOWLEDGMENTS

The authors are very grateful for the financial support from AFOSR (FA9550-12-1-0069) under the Polymer Chemistry Task in the Directorate of Chemistry and Life Sciences (Dr. Charles Lee, Program Manager). Partial support from the Wenzhou Medical College, the Zhejiang Innovation Team from the Department of Education (T200917), the Ministry of Education of China (IRT1077, 211069, and 20103321120003), and the National "Thousand Talents Program" of China, the Ministry of Science and Technology of China (2009DFB30380), and NSFC-NSF MWN (NSF-DMR 1106160) is also acknowledged.

## ■ REFERENCES

(1) Novoselov, K. S.; Geim, A. K.; Morozov, S. V.; Jiang, D.; Zhang, Y.; Dubonos, S. V.; Grigorieva, I. V.; Firsov, A. A. Electric Field Effect in Atomically Thin Carbon Films. *Science* **2004**, *306*, 666−669.

(2) Allen, M. J.; Tung, V. C.; Kaner, R. B. Honeycomb Carbon: A Review of Graphene. *Chem. Rev.* **2010**, *110*, 132−145.

(3) Yu, D.; Negelli, E.; Naik, R.; Dai, L. Asymmetrically Functionalized Graphene for Photodependent Diode Rectifying Behavior. *Angew. Chem., Int. Ed.* **2011**, *50*, 6575−6578.

(4) Yu, D.; Yang, Y.; Durstock, M.; Baek, J.-B.; Dai, L. Soluble P3HT-Grafted Graphene for Efficient Bilayer−Heterojunction Photovoltaic Devices. *ACS Nano* **2010**, *4*, 5633−5640.

(5) Qu, L.; Liu, Y.; Baek, J. B.; Dai, L. Nitrogen-Doped Graphene as Efficient Metal-Free Electrocatalyst for Oxygen Reduction in Fuel Cells. *ACS Nano* **2010**, *4*, 1321−1326.

(6) Xie, X.; Qu, L.; Zhou, C.; Li, Y.; Zhu, J.; Bai, H.; Shi, G.; Dai, L. An Asymmetrically Surface-Modified Graphene Film Electrochemical Actuator. *ACS Nano* **2010**, *4*, 6050−6054.

(7) Guo, C. X.; Guai, G. H.; Li, C. M. Graphene Based Materials: Enhancing Solar Energy Harvesting. *Adv. Energy Mater.* **2011**, *1*, 448−452.

(8) Xue, Y.; Chen, H.; Yu, D.; Wang, S.; Yardeni, M.; Dai, Q.; Liu, Y.; Qu, J.; Dai, L. Oxidizing Metal Ions with Graphene Oxide: The *in-situ* Formation of Magnetic Nanoparticles on Self-Reduced Graphene Sheets for Multifunctional Applications. *Chem. Commun.* **2011**, *47*, 11689−11691.

(9) Choi, E.-K.; Jeon, I.-Y.; Bae, S.-Y.; Lee, H.-J.; Shin, H. S.; Dai, L.; Baek, J.-B. High-Yield Exfoliation of Three-Dimensional Graphite into Two-Dimensional Graphene-like Sheets. *Chem. Commun.* **2010**, *46*, 6320−6322.

(10) Bae, S.-Y.; Jeon, I.-Y.; Yang, J.; Park, S.; Park, N.; Shin, H. S.; Park, S.; Ruoff, R. S.; Dai, L.; Baek, J.-B. Large-Area Graphene Films by Simple Solution Casting of Edge-Selectively Functionalized Graphite. *ACS Nano* **2011**, *5*, 4974−4980.

(11) Jeon, I.-Y.; Bae, S.-Y.; Yu, D.; Chang, D. W.; Dai, L.; Baek, J.-B. Formation of Large-Area Nitrogen-Doped Graphene Film Prepared from Simple Solution Casting of Edge-Selectively Functionalized Graphite and Its Electrocatalytic Activity. *Chem. Mater.* **2011**, *23*, 3987−3992.

(12) Yu, G.; Gao, J.; Hummelen, J. C.; Wudl, F.; Heeger, A. J. Polymer Photovoltaic Cells: Enhanced Efficiencies via a Network of Internal Donor−Acceptor Heterojunctions. *Science* **1995**, *270*, 1789−1791.

(13) Li, G.; Shrotriya, V.; Huang, J.; Yao, Y.; Moriarty, T.; Emery, K.; Yang, Y. High-Efficiency Solution Processable Polymer Photovoltaic Cells by Self-Organization of Polymer blends. *Nat. Mater.* **2005**, *4*, 864−868.

(14) Thompson, B. C.; Fréchet, J. M. J. Polymer−Fullerene Composite Solar Cells. *Angew. Chem., Int. Ed.* **2008**, *47*, 58−77.

(15) Steim, R.; Koglera, F. R.; Brabec, C. J. Interface Materials for Organic Solar Cells. *J. Mater. Chem.* **2010**, *20*, 2499−2512.

(16) Park, J. H.; Lee, T.-W.; Chin, B.-D.; Wang, D. H.; Park, O. O. Roles of Interlayers in Efficient Organic Photovoltaic Devices. *Macromol. Rapid Commun.* **2010**, *31*, 2095−2108.

(17) Kim, Y.-H.; Lee, S.-H.; Noh, J.; Han, S.-H. Performance and Stability of Electroluminescent Device with Self-Assembled Layers of Poly(3,4-ethylenedioxythiophene)−Poly(styrenesulfonate) and Poly-electrolytes. *Thin Solid Films* **2006**, *510*, 305−310.

(18) Kemerink, M.; Timpanaro, S.; de Kok, M. M.; Meulenkamp, E. A.; Touwslager, F. J. Three-Dimensional Inhomogeneities in PEDOT:PSS Films. *J. Phys. Chem. B* **2004**, *108*, 18820−18825.

(19) Shrotriya, V.; Li, G.; Yao, Y.; Chu, C. W.; Yang, Y. Transition Metal Oxides as the Buffer Layer for Polymer Photovoltaic Cells. *Appl. Phys. Lett.* **2006**, *88*, 073508−073508−3.

(20) Liao, H.-H.; Chen, L.-M.; Xu, Z.; Li, G.; Yang, Y. Highly Efficient Inverted Polymer Solar Cell by Low Temperature Annealing of $Cs_2CO_3$ Interlayer. *Appl. Phys. Lett.* **2008**, *92*, 173303−173303−3.

(21) Irwin, M. D.; Buchholz, D. B.; Hains, A. W.; Chang, R. P. H.; Marks, T. J. *p*-Type Semiconducting Nickel Oxide as an Efficiency-Enhancing Anode Interfacial Layer in Polymer Bulk-Heterojunction Solar Cells. *Proc. Natl. Acad. Sci. U.S.A.* **2008**, *105*, 2783−2787.

(22) Chan, M. Y.; Lee, C. S.; Lai, S. L.; Fung, M. K.; Wong, F. L.; Sun, H. Y.; Lau, K. M.; Lee, S. T. Efficient Organic Photovoltaic Devices Using a Combination of Exciton Blocking Layer and Anodic Buffer Layer. *Appl. Phys. Lett.* **2006**, *100*, 094506-1−094506-4.

(23) Li, S. S.; Tu, K. H.; Lin, C. C.; Chen, C. W.; Chhowalla, M. Solution-Processable Graphene Oxide as an Efficient Hole Transport Layer in Polymer Solar Cells. *ACS Nano* **2010**, *4*, 3169−3174.

(24) Gao, Y.; Yip, H. L.; Hau, S. K.; O'Malle, K. M.; Cho, N.; Chen, H. Z.; Jen, A. K. Y. Anode Modification of Inverted Polymer Solar Cells Using Graphene Oxide. *Appl. Phys. Lett.* **2010**, *97*, 203306-1−203306-3.

(25) Gao, Y.; Yip, H. L.; Chen, K.-S.; O'Malle, K.; Acton, M. O.; Sun, Y.; Ting, G.; Chen, H. Z.; Jen, A. K. Y. Surface Doping of Conjugated Polymers by Graphene Oxide and Its Application for Organic Electronic Devices. *Adv. Mater.* **2011**, *23*, 1903−1908.

(26) Yeo, S.; Kim, J.; Jeong, H.-G.; Kim, D.-Y.; Noh, Y.-J.; Kim, S.-S.; Ku, B.-C.; Na, S.-I. Solution-Processable Reduced Graphene Oxide as a Novel Alternative to PEDOT:PSS Hole Transport Layers for Highly

Efficient and Stable Polymer Solar Cells. *Adv. Mater.* **2011**, *23*, 4923−4928.
(27) Liu, J.; Xue, Y.; Gao, Y.; Yu, D.; Durstock, M.; Dai, L. Hole and Electron Extraction Layers Based on Graphene Oxide Derivatives for High-Performance Bulk Heterojunction Solar Cells. *Adv. Mater.* **2012**, *24*, 2228−2233.
(28) Eda, G.; Chhowalla, M. Chemically Derived Graphene Oxide: Towards Large-Area Thin-Film Electronics and Optoelectronics. *Adv. Mater.* **2010**, *22*, 2392−2415.
(29) Dreyer, D. R.; Park, S.; Bielawski, C. W.; Ruoff, R. S. The Chemistry of Graphene Oxide. *Chem. Soc. Rev.* **2010**, *39*, 228−240.
(30) Si, Y. C.; Samulski, E. T. Synthesis of Water Soluble Graphene. *Nano Lett.* **2008**, *8*, 1679−1682.
(31) Zhao, G.; Jiang, L.; He, Y.; Li, J.; Dong, H.; Wang, X.; Hu, W. Sulfonated Graphene for Persistent Aromatic Pollutant Management. *Adv. Mater.* **2011**, *23*, 3959−3963.
(32) Dang, M. T.; Hirsch, L.; Wantz, G. P3HT:PCBM, Best Seller in Polymer Photovoltaic Research. *Adv. Mater.* **2011**, *23*, 3597−3602.
(33) Chiang, L. Y.; Wang, L.-Y.; Swirczewski, J. W.; Soled, S.; Cameron, S. Efficient Synthesis of Polyhydroxylated Fullerene Derivatives via Hydrolysis of Polycyclosulfated Precursors. *J. Org. Chem.* **1994**, *59*, 3960−3968.
(34) Dai, L.; Lu, J.; Matthews, B.; Mao, A. W. H. Doping of Conducting Polymers by Sulfonated Fullerene Derivatives and Dendrimers. *J. Phys. Chem. B* **1998**, *102*, 4049−4053.
(35) Wei, Z.; Wan, M.; Lin, T.; Dai, L. Polyaniline Nanotubes Doped with Sulfonated Carbon Nanotubes Made via a Self-Assembly Process. *Adv. Mater.* **2003**, *15*, 136−139.
(36) Gao, W.; Alemany, L. B.; Ci, L.; Ajayan, P. M. New Insights into the Structure and Reduction of Graphite Oxide. *Nat. Chem.* **2009**, *1*, 403−408.
(37) Stankovich, S.; Dikin, D. A.; Piner, R. D.; Kohlhaas, K. A.; Kleinhammes, A.; Jia, Y.; Wu, Y.; Nguyen, S. T.; Ruoff, R. S. Synthesis of Graphene-Based Nanosheets via Chemical Reduction of Exfoliated Graphite Oxide. *Carbon* **2007**, *45*, 1558−1565.
(38) Pei, S.; Zhao, J.; Du, J.; Ren, W.; Cheng, H. Direct Reduction of Graphene Oxide Films into Highly Conductive and Flexible Graphene Films by Hydrohalic Acids. *Carbon* **2010**, *48*, 4466−4474.